Atmos. Chem. Phys., 11, 1473–1490, 2011
www.atmos-chem-phys.net/11/1473/2011/
doi:10.5194/acp-11-1473-2011

Atmospheric Chemistry and Physics

Oxygen isotopic signature of CO_2 from combustion processes

M. Schumacher[1,2,3], R. A. Werner[3], H. A. J. Meijer[1], H. G. Jansen[1], W. A. Brand[2], H. Geilmann[2], and R. E. M. Neubert[1]

[1]Centre for Isotope Research, University of Groningen, Nijenborgh 4, 9747 AG Groningen, The Netherlands
[2]Max-Planck-Institute for Biogeochemistry, Hans-Knoell-Straße 10, 07745, Jena, Germany
[3]Institute of Plant Sciences, Swiss Federal Institute of Technology Zürich, Universitätsstraße 2, 8092 Zürich, Switzerland

Received: 21 July 2008 – Published in Atmos. Chem. Phys. Discuss.: 5 November 2008
Revised: 2 February 2011 – Accepted: 5 February 2011 – Published: 16 February 2011

Abstract. For a comprehensive understanding of the global carbon cycle precise knowledge of all processes is necessary. Stable isotope (^{13}C and ^{18}O) abundances provide information for the qualification and the quantification of the diverse source and sink processes. This study focuses on the $\delta^{18}O$ signature of CO_2 from combustion processes, which are widely present both naturally (wild fires), and human induced (fossil fuel combustion, biomass burning) in the carbon cycle. All these combustion processes use atmospheric oxygen, of which the isotopic signature is assumed to be constant with time throughout the whole atmosphere. The combustion is generally presumed to take place at high temperatures, thus minimizing isotopic fractionation. Therefore it is generally supposed that the ^{18}O signature of the produced CO_2 is equal to that of the atmospheric oxygen. This study, however, reveals that the situation is much more complicated and that important fractionation effects do occur. From laboratory studies fractionation effects on the order of up to 26‰ became obvious in the derived CO_2 from combustion of different kinds of material, a clear differentiation of about 7‰ was also found in car exhausts which were sampled directly under ambient atmospheric conditions.

We investigated a wide range of materials (both different raw materials and similar materials with different inherent ^{18}O signature), sample geometries (e.g. texture and surface-volume ratios) and combustion circumstances. We found that the main factor influencing the specific isotopic signatures of the combustion-derived CO_2 and of the concomitantly released oxygen-containing side products, is the case-specific rate of combustion. This points firmly into the direction of (diffusive) transport of oxygen to the reaction zone as the cause of the isotope fractionation. The original total ^{18}O signature of the material appeared to have little influence, however, a contribution of specific bio-chemical compounds to individual combustion products released from the involved material became obvious.

Correspondence to: M. Schumacher
(marcus.schumacher1@gmx.net)

1 Introduction

The contribution from both natural and human-induced biomass burning and from fossil fuel combustion to the annual total carbon flux between the land surface and the atmosphere is estimated to be approximately 2.5% and 6%, respectively (IPCC, 2007). Yet, they form a considerable part of the actual anthropogenic disturbance of the global carbon cycle with fossil fuel combustion increasing steadily.

1.1 The combustion issue – why do we need this information?

The main CO_2 emissions from fossil fuel can be found in the highly industrialised countries and in countries with economies in transition, mainly located in the northern hemisphere. The contribution shows a slight seasonality since public electricity and heat production are the largest CO_2 emission sources (IEA, 2005). In developing countries a non-negligible source of CO_2 is the domestic combustion of biomass fuels (Kituyi et al., 2001; Ludwig et al., 2003). Regularly, large wild fires occur during the summer or dry season in such areas as the boreal forest zones of Russia and Canada (Goldammer and Furyaev, 1996; Kasischke et al., 2005), in the forests and shrub lands of the Mediterranean, and in the tropical forests (Hao and Liu, 1994). In addition peat

lands (Page et al., 2002) and the savannas are ignited either naturally or intentionally for the cultivation of arable land. The inter-annual variability of fire counts and the amount of carbon released during these events is high. For the eight year observation period from 1997 to 2004 Van der Werf et al. (2006) report a range from a minimum of 2.0 Pg C yr^{-1} in 2000 to the maximum of 3.2 Pg C yr^{-1} in 1998. Even if fires are in principle local to regional events, a global impact due to atmospheric transport is observed (Damoah et al., 2004).

Within the global carbon cycle the atmosphere acts as a link between the oceans and the terrestrial biosphere/anthroposphere. Characteristic exchange processes can be distinguished by their fingerprints, identified for instance by trace gas compositions and the stable isotope ratios of CO_2 – i.e. the isotope ratios of its elements carbon and oxygen. One of the topics where isotopic studies can be of help is the location of the formerly so-called "missing carbon sink" (Prentice et al., 2000). That is to verify the interannually and regionally varying sink partitioning of the anthropogenic disturbance of the carbon cycle, i.e. the respective part of CO_2 derived from fossil fuel combustion and land use change, that is taken up by the reservoirs biosphere, ocean and atmosphere. For achieving this task, carbon cycle models are an important tool. However, a mandatory requirement to satisfy the challenge is to know all input data, e.g. the isotopic signatures derived from different processes, with a high precision.

In order to understand the global carbon cycle, more detailed information about the amounts of anthropogenic emissions from the utilization of fossil fuels and the contribution due to the consumption of biomass is necessary. The main sources of knowledge about fossil fuels are sales statistics. However, sale and actual combustion do not always take place instantly and at the same place. In addition, independent verification of the emission reductions is required from the contract parties of the UNFCCC Kyoto protocol.

1.2 Status of knowledge and hypothesis about $\delta^{18}O$ of combustion-derived CO_2

Between the relating isotopes in CO_2 major differences can be seen in the diverse source and sink processes. While the biospheric ^{13}C signal mostly depends on the plant physiology, the activity and the environmental conditions during CO_2 uptake, and accordingly on the plant material consumed by combustion or microbial decay, ^{18}O in CO_2 is closely connected to the water cycle. The global $\delta^{18}O$ background signal of CO_2 is set by atmosphere-ocean CO_2 exchange, and modified on land by the interaction with the vegetation (Ciais and Meijer, 1998). Because the ^{18}O containing molecules are characterized by a lower evaporation rate than the light ones (without ^{18}O), they tend to remain in liquid water, rain out faster from clouds, and are thus reduced in aged clouds. Thereby a gradient is actively maintained (primarily for water and by ongoing isotope-exchange also for CO_2) that shows a depletion of the ^{18}O isotope on a transect from the tropics to the poles, and also over the continents along the same latitude with increasing distance inland (Rayleigh-distillation, Francey and Tans, 1987). Further on, regional differences are induced since the oxygen signal of plant water and plant material is strongly related to the oxygen isotope ratio in rain and groundwater. Due to plant-physiological processes and fractionation coupled to transpiration, the plant leaf water is distinctly enriched in ^{18}O compared to the source water (Burk and Stuiver, 1981). The modulation of the CO_2-$\delta^{18}O$ background signal takes place by exchange with the enriched oxygen of plant leaf water when CO_2 enters the stomata and leaves again without being assimilated (Farquhar et al., 1993). Isotope discrimination in plant metabolism occurs during biosynthesis of carbohydrates and other primary or secondary products; e.g. Sternberg (1989) describes for cellulose oxygen isotope ratios to be 27‰ (±3‰) higher relative to leaf water. Caused by further kinetic and equilibrium isotopic effects, the $\delta^{18}O$ value decreases for secondary products; total plant dry matter has a $\delta^{18}O$ value of about 18‰ (Yakir, 1998). Thus, it might well be that the material's oxygen isotope signature in particular with respect to specific compounds influences the combustion products to some extent.

A differentiation between CO_2 originating from respiration and from biomass burning solely by measuring CO_2 and its $\delta^{13}C$ is hardly feasible. One approach postulated is the utilization of multispecies analyses (Langenfelds et al., 2002; Schumacher, 2005), taking other trace gases into account that accompany combustion processes but are not formed by respiration. However, if a probable separation by the $\delta^{18}O$ signal in CO_2 is detectable, an additional useful tool would become available.

Thus, the main questions of this study are: (1) does combustion-derived CO_2 vary isotopically due to the type of the burnt material (e.g. needles, wood, lichen, shrubs, heather)? (2) Can we distinguish anthropogenic contributions formed by the consumption of fossil fuels from emissions of biomass burning? And does the actual kind of the biomass lead to individual isotopic characteristics? (3) Is a separation with respect to the wildfire type (i.e. smoldering peat land to explosive crown fires) possible?

Until now, for all combustion-derived CO_2 a $\delta^{18}O$ of −17‰ (w.r.t. VPDB- CO_2) is used in the recent carbon cycle isotope models (e.g. Ciais et al., 1997a, b), derived from the isotopic ratio in atmospheric molecular oxygen as given by Kroopnick and Craig (1972) to be 23.5‰ on the SMOW-scale, which was later corrected to 23.8‰ w.r.t. VSMOW (Coplen, 1988; USGS, 2002; the value on the VPDB-CO_2 scale then is −16.98‰). There are theoretical doubts as well as experimental evidences (Zimnoch, 1996; Pataki et al., 2003; Zimnoch et al., 2004) questioning the validity of this hypothesis under different circumstances. The value of 23.8‰ VSMOW (−17‰ VPDB-CO_2) is derived from a complete and thus unfractionated usage of the involved

(atmospheric) oxygen, i.e. the full transfer of the isotope signature. To ensure this, a closed combustion volume and a good control on the combustion mode are necessary, which is mostly given for advanced combustion machines. However, open fires, i.e. fires with an unlimited O_2 availability, always include a diffusive step in the supply of oxygen to the actual combustion spot. This is a mass-fractionation sensitive process where the heavier isotopes are expected to be depleted in the combustion-derived CO_2. The combustion process itself does most likely not give rise to fractionation effects, because of the fast reactions due to the high temperatures. There is, however, always a partitioning of the oxygen involved, as the formed oxygen containing products (e.g. CO_2, H_2O, CO) do not carry exactly the same isotopic signature.

All isotopic data are expressed in the common δ nomenclature, expressing the relative deviation of the sample $^{18}O/^{16}O$ ratio from a reference isotopic ratio in per mill (‰).

$$\delta^{18}O_{VPDB-CO_2}/‰ = ((R_{sample}/R_{VPDB-CO_2}) - 1) \cdot 1000 \quad (1)$$

The primary international standard for the oxygen isotopic variation in natural compounds is VSMOW (Vienna Standard Mean Ocean Water). Independent from this standard (but closely coupled with it) the oxygen isotopic signature is often also specified on the VPDB-CO_2 carbonate scale (Vienna Peedee Belemnite derived CO_2). The conversion factors from the VSMOW to the VPDB-CO_2 scale and vice versa are given in Werner and Brand (2001).

Depending on the kind of the combusted material and the type of the combustion process, characteristic signals with respect to the trace gas composition and the isotopic ratio of the formed gases are expected. For the oxygen isotopes in the formed combustion CO_2 this can be described by the general formula:

$$(C-O-R_{fuel}) + O_2 \rightarrow CO + CO_2 + H_2O + R_{oxy} + O_2 \quad (R1)$$

with the first term on the left side in brackets representing the input material, and R_{oxy} on the right hand site being a substitute for additional oxidized compounds of the fuel.

1.3 Combustion parameters

The burning process can be separated into three phases: (1) the heating of the material – that provokes the degassing of volatile compounds – to a certain temperature at which the ignition happens (if sufficient oxygen is available). (2) Under continuous support of oxygen and of flammable gases, mainly from the thermal decomposition of hydrocarbons, a direct oxidation of the fuel gas occurs with the formation of an open flame. (3) In particular the less thermally degradable compounds are processed within the third phase. Both this third phase, usually called smoldering, and the first step are characterized by the absence of an open flame. The burning regimes and the relevant combustion processes are summarized in Table 1.

1.4 Conceptual approach and investigation strategy

To study the influence of effective parameters for combustion, the experiments on CO_2 isotopic signature were carried out both under controlled laboratory conditions, and as field sampling. The main parameters which we focussed on were: (1) type of fuel, (2) structure of the material, (3) oxygen availability, (4) combustion temperature, (5) water content and (6) composition of the atmosphere under which the combustion takes place. Besides the carbon and oxygen isotope signature in the derived CO_2 also the δD and $\delta^{18}O$ values in the combustion water were determined for selected samples.

From a pool covering a broad band of fuel types (e.g. wood, needles, lichen, shrubs, peat, coal, lignite, natural gas) a subset of 35 samples was chosen to be burnt with respect to the addressed questions. The main motivation for this selection was to examine the influence of the chemical composition and structure of the material. We expected a broad differentiation between the fuels due to the relative and absolute amount of the material's inherent oxygen and the resulting different oxidative ratios. To give an example we compare coal $C_{200}H_{120}O_5N_3S$ to cellulose $C_6H_{10}O_5$. For the production of 1 molecule CO_2 from the complete combustion of coal 1.975 oxygen atoms from the ambient air are needed versus 1.167 for cellulose when forming solely CO_2, and accordingly 2.3 oxygen atoms from ambient air (= 1.15 mol O_2/mol CO_2) for coal and 2.0 oxygen atoms from ambient air (= 1.0 mol O_2/mol CO_2) for cellulose when taking the formation of further side products like H_2O, NO and SO_2 into consideration.

Additionally one has to take into account the diversity of the isotopic signature of the fuel oxygen that varies for material from different locations. Another diverging influence was anticipated due to the structure of the solid fuels, influencing mainly the heat conductance and the disaggregation of the substance. Therefore selected samples were combusted both as solid cubic fuel sample as well as ground to a smaller grain size.

The water content of the material should be of some importance with respect to the burning process, because of the energy consumption for evaporation which reduces the combustion temperature, but also as probable exchange partner for the oxygen (isotopes) in CO_2 when condensing in the cooling smoke plume. This hypothesis was tested by comparing the isotopic composition of CO_2 produced from dry and wetted material. Selected solid fuels were therefore wetted for three days until the material was completely soaked in two waters of distinct isotopic composition, one from the Atlantic Ocean ($\delta^{18}O = 0.5$‰ VSMOW, $\delta D = 28.2$‰ VSMOW) and one from Antarctica ($\delta^{18}O = -43.7$‰ VSMOW, $\delta D = -346.1$‰ VSMOW).

It was assumed that the combustion temperature is a main criterion for the burning regime and that it has a major influence on the disaggregating of the material. Therefore, a specific experiment series was conducted examining the isotopic

Table 1. General schematics of the burning regimes, the oxygen sources, material characteristics, the relevant combustion processes and of the formed substances. Depending on the kind of material, the environmental conditions and the burning behaviour the contribution of oxygen from the different sources and the formed products are variable.

Burning Regime	Oxygen Source	Material Characteristics	Reaction Processes		Formed Substances
Degassing (≤ 270 °C for plant material) (≤480 °C for coal, charcoal)	Structure material	Species, part → elemental & structural composition	Release of volatile (organic) components		VOCs, H_2O, CO, CH_4, NO_x, CO_2 Black carbon
	Cellular water	Wilting coefficient	Deprivation of energy for evaporation	↓ PROGRESSION OF THE DECOMPOSITION FRONT ↓	
	Ambient air		Accessibility to material surface & burning gases		
Open flame Natural conditions: (≤570 °C for plant material) (≤700 °C for coal, charcoal)	Ambient air		Accessibility to material surface & burning gases ↯ Transport of mass and heat Reaction velocity/size of the zone where burning can happen determines the efficiency of the conversion process, i.e. the release of incompletely oxidized combustion products		CO_2, CO → CO_2 (needs Temp. >600 °C) H_2O Black carbon
Optimal conditions:	Structure material	Species, part → more stable components (Lignin, etc.)	Decomposition of less volatile components and of skeletal structure		
≥ 650 °C	Cellular water		Deprivation of energy for evaporation		
Glowing/ Smoldering	Ambient air		Accessibility to material surface & burning gases		CO_2, CO, H_2O Black carbon
(≥600 °C down to 120–350 °C)	Structure material	Thermally converted source material	Decomposition of skeletal structure (charcoal shell); all volatiles expelled		

signatures related to distinct maximum temperatures. Identical material samples were heated each to a maximum temperature of 450 °C, 600 °C and 750 °C for needle and wood material, and accordingly 500 °C and 750 °C for fossil fuels and the oven temperature maintained on this level until the termination of the experimental time.

A final focus was put on the availability of oxygen, which is on the one hand side regulated by the theoretical pool for the combustion reaction (sum of the mixing ratio in the air and the fuel oxygen) and on the other side by the amount of the effectively usable oxygen, depending on the removal of combustion products, the direct supply of oxygen by diffusion and the interaction with different gases. To study the effect of variable oxygen availability a test series using well-known cellulose standard material (IAEA-C3; Buhay et al., 1995) was carried out. The oxygen flow rate was reduced, which concomitantly resulted in a decreased removal of the combustion products. Additional information was expected from the combustion experiments using atmospheric air with ambient oxygen content and isotopic signature ($\delta^{18}O = 23.8‰$ VSMOW/−17‰ VPDB-CO_2), as compared to the admission of pure oxygen.

2 Material and methods

The laboratory combustion system for the solid samples consists of three parts. (1) Oxygen supply, (2) the combustion section and (3) the CO_2 extraction (see Fig. 1).

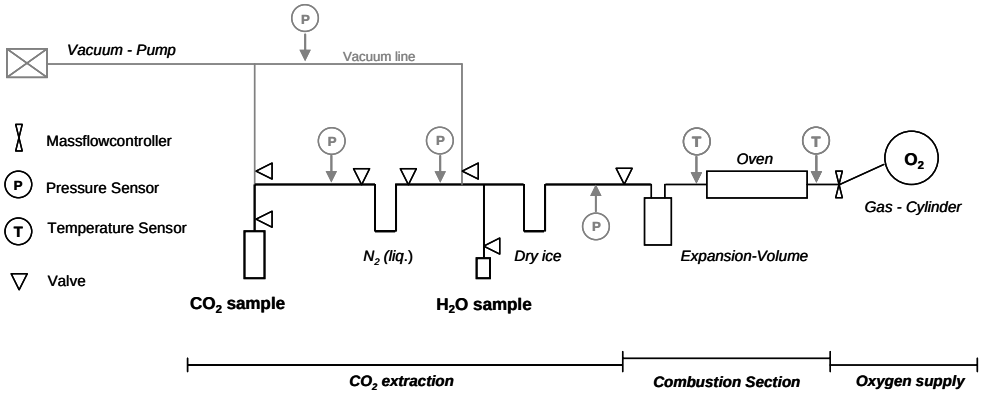

Fig. 1. Sketch of the technical set-up. For detailed description see text.

In order to create optimal burning conditions, pure oxygen was applied with an amount ten times higher than the stoichiometrically calculated consumption for complete combustion. Therefore oxygen "5.0" of 99.999% purity ($\delta^{18}O = 27.2‰$ VSMOW, Hoek-Loos, Schiedam, NL) was fed from the cylinder via a mass flow-controller (MKS Instruments) into the combustion tube (quartz glass encapsulated by an electrical oven). Two temperature sensors were applied in front of and behind the sample, which was inserted into the tube on a small sliding shuttle (also quartz glass). The combustion section was separated in direction to the oxygen cylinder by a two-port stainless-steel valve (Swagelok) and to the extraction compartment by a glass valve sealed with viton o-rings (as for all connections in this line). An additional expansion volume of 600 ml was connected to the combustion tube, in order to allow the collection of the exhaust gas for each sample at a single "blow". The combustion process followed for all experiments a similar scheme (see also Fig. 1): after inserting the sample the complete system was evacuated. Then the CO_2 extraction compartment was separated from the combustion section by closing the connection valve. Concomitant with the heating of the electric oven (controlled by a voltage transformer at 170 V) the oxygen supply was enabled. After about 17 s a temperature of 250 °C was reached, 650 °C was exceeded after roughly 65 s. After reaching the target temperature this was maintained by manual control of the oven voltage until the end of the experiment at 120 s. Then the power supply for the oven was switched off and the oxygen supply was interrupted. When the temperature had dropped down to 500 °C the valve to the CO_2 extraction section was opened and the combustion gas directed through the cold traps. To extract the CO_2, a first cryogenic trap cooled with dry ice-alcohol slush removed constituents with condensing temperatures above −78 °C, ensuring that no liquid water remained, which might affect the results by oxygen isotope exchange (Gemery et al., 1996). In the second liquid nitrogen cooled trap the CO_2 was frozen out at −196 °C in 50 ml glass flasks, and accordingly in 100 ml glass flasks for specific series, like the "water experiment". Within the separation section and the sampling flasks a vacuum of 10 mPa was maintained.

A similar technical design was also used for the combustion of the natural gas, except the combustion section where a welding torch (as used for oxyacetylene welding) was applied, connected to the natural gas and the oxygen lines, thus both gases were mixed directly before combustion. The flame was encapsulated within a glass dome (1 L volume) that was linked via a three-port stainless-steel valve (Swagelok) to the extraction compartment. To remove all ambient air from the glass dome the exhaust was released to the laboratory extractor hood for at least three minutes before the combustion gases were allowed to enter the extraction compartment by switching the valve.

For the laboratory experiment focussing on the fractionation signal in ambient atmospheric air, the oxygen cylinder was replaced by a cylinder containing air sampled at the monitoring station "Lutjewad", operated by Centre for Isotope Research (CIO) at the North coast of the Netherlands ($\delta^{18}O = 23.8‰$ VSMOW/−17‰ VPDB-CO_2).

To perform the sampling of car exhaust under ambient atmospheric conditions a simple system was developed consisting of (1) an inlet section and (2) an evacuated 2.5 L glass flask. By a small pump (N 814 KNDC, KNF Neuberger) sample air was sucked in through a tube protected by a 2 µm particle filter (Swagelok) that was inserted into the exhaust of the car. The air flowed through Dekabon tubing via a cryotrap filled with dry ice-alcohol slush (in order to remove water and other easily condensable constituents) to a three-port valve (stainless-steel; Swagelok). The direct line was connected to the evacuated glass flask while the third port connected the whole system with the pump. After flushing the system for a while with the car exhaust the connection to the pump was closed and the sample was taken by replenishing the glass flask. Immediately after the sampling was finished the flasks were brought to the laboratory and connected to the CO_2 extraction system of the laboratory setup.

2.1 Description of the analytical equipment

All combustion-derived CO_2 samples were analyzed for their $\delta^{18}O$ and $\delta^{13}C$ in Groningen on CIO's Micromass SIRA-10 dual-inlet isotope ratio mass spectrometer. The determination of the cross-contamination correction has been described by Meijer et al. (2000). A routine precision of ± 0.05‰ for $\delta^{18}O$ and ± 0.03‰ for $\delta^{13}C$ is achieved.

The examination of the fuel materials' inherent $\delta^{13}C$ and $\delta^{18}O$ was performed at the Isolab of the MPI-BGC in Jena. To define the bulk ^{18}O the sample was "pyrolized" (carbon reduction) to CO using a high temperature pyrolysis reactor with a "tube in tube" design (glassy carbon in a silicium carbide tube, "HTO" HEKAtech GmbH; equipped with a zero blank auto sampler, Costech Analytical Technologies and an additional reversed He feed, Gehre et al., 2004). Via a ConFlo III interface (Thermo Finnigan) the reactor was coupled to the isotope ratio mass spectrometer (Delta plus XL, Thermo Finnigian), performing the measurements of samples, blanks and standards after Werner and Brand (2001). The normalized results (Coplen, 1988) achieve a routine precision of ± 0.1‰ $\delta^{18}O$.

$\delta^{13}C$ values were obtained by using a Flash NA 1110 Series elemental analyzer (Thermo Italy) coupled via a ConFlo III interface to the DeltaC isotope ratio mass spectrometer (Thermo Finnigan).

For the oxygen and hydrogen isotope analysis of the combustion-derived water samples, a similar pyrolysis reactor with a "tube in tube" design (glassy carbon in an aluminium oxide tube) was applied in Groningen like it has been in Jena for the bulk material $\delta^{18}O$. The $\delta^{18}O$ and $\delta^{2}H$ measurements are performed in batches using a HEKAtech High Temperature Pyrolysis unit (Gehre and Strauch, 2003; Gehre et al., 2004) in which the injected water is reacting, using the glassy carbon available in the reactor, according to:

$$H_2O + C \rightarrow H_2 + CO \quad \text{(R2)}$$

The H_2 and CO gas, emerging into a continuous Helium flow through the system, are then led through a GC column to separate the two gases in time, and fed into a GVI Isoprime Isotope Ratio Mass Spectrometer for the actual isotope ratio analysis.

For a full analysis of both $\delta^{2}H$ (from the H_2 gas, emerging first from the GC column) and $\delta^{18}O$ (from the CO gas) every sample is injected typically 9 times from the same vial into the HT furnace, in 0.2 µl aliquots. The first five injections are used for $\delta^{2}H$ exclusively, the sixth is used for both $\delta^{2}H$ and $\delta^{18}O$ (by switching the mass detection of the IRMS at the proper time), and the final three are used only for $\delta^{18}O$.

In our injection scheme, the memory effects of the HTO oven, that are important here due to the small injection volumes and the large range of the isotopic signal, can be accurately corrected for, using a memory correction algorithm similar to the one described by Olsen et al. (2006). The isotope scales are calibrated using multiple samples of two internal standard waters, being at the lower and higher end of the sample range, respectively, and with well-known isotope values from "classical" high-volume analysis techniques, whereas the measured values for a third standard, of which the value is in the midrange of the samples, is used as quality "target". The routine precision achieved was ± 0.2‰ for $\delta^{18}O$ and $< \pm 1$‰ for $\delta^{2}H$.

2.2 Selection and preparation of the fuel material

For the combustion a large pool of different kinds of material was available. Biomass samples covering duff, shrub and tree material and fossil fuels comprising peat, lignite, coal, charcoal and crude oil. Most of the biomass samples were at hand as identical species from different locations, mostly even from the same growing years. Part of this could be easily achieved through the use of Christmas trees (harvest 2004) of uniform age structure. To ensure the comparability of samples from non-Christmas trees only needles were used from the year 2004. For the compared wood fuel intercepts covering the years 1960–1995 were selected.

All samples were cleaned from adherent impurities and dried until mass constancy at 30 °C to avoid the release of volatile compounds already when drying. For the combustion bulk fuel was weighted in to the sliding shuttle. The amount for the different materials depended on the capacity of the collecting bin and the calculated CO_2 gain within the range between coal (20 mg) and plant material (35 mg), and accordingly 70 mg for the "dry" plant material used in the wetness experiment to ensure enough production of combustion derived water for analysis. Wood samples were cut in thin slides as radial sections without contributions from bark and cambium. Because of the different growth rates of the various tree types the sections were also variable in length and thickness. Needles were combusted as a whole packed as a set of several individual needles of different size. From the bark a cube was cut and tailored to fit the calculated weight, the samples for the fossil fuels were handled in the same way. In order to study the impact of the material's structure, for some fossil fuel samples additional material with small grain size was prepared. The heather samples were composed each of a twig with leafs and flowers shortened to the appropriate length. Each lichen sample consisted of one part of a lobe trimmed to fit the weight. The cellulose samples were cut off from one single board of reference material (IAEA-C3) in the shape of a rectangle. For the wetness experiment one solid block of 70 mg was prepared. In contrast, the wood material consisted of two separated stripes for this experiment.

For the determination of the fuel $\delta^{18}O$ the material was ground and homogenized. The samples were weighed out to Ag capsules and dropped via the auto sampler into the HTO.

To evaluate the variance due to factors related to the performance of the experiments we carried out test combustions with the homogeneous cellulose material. We compared for this purpose two samples each from combustions

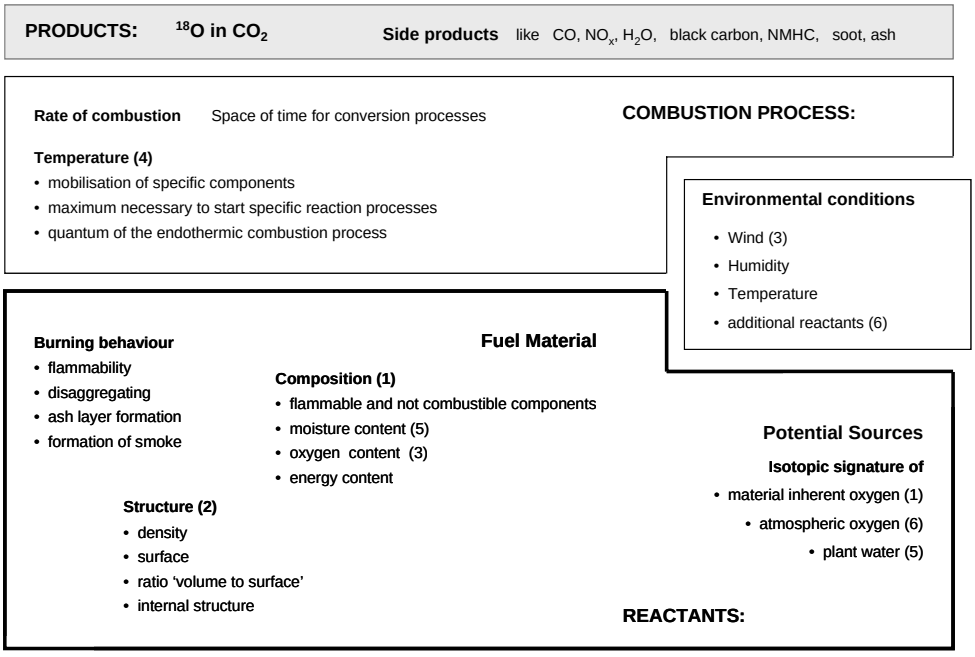

Fig. 2. Major aspects and interactions relevant for combustion processes. The numbers in brackets indicate the several factors focussed on by the specific experiments.

with different oxygen provision. The difference of the samples performed with low oxygen provision was 0.235‰, the difference with high oxygen support was 0.070‰. The analytical variance between replicates is thus distinctly smaller than the biological variance that was observed between samples from the same location but different pine trees (see Fig. 3 "Pine Siberia I and II"; $\Delta = 0.693$‰).

3 Results and discussion

The initial goal of this study was to investigate whether the oxygen isotopic signature of combustion-derived CO_2 is determined solely by the $\delta^{18}O$ of atmospheric oxygen, or how far it depends on factors like (1) the type of fuel, (2) structure of the material, (3) oxygen availability, (4) combustion temperature, (5) water content and (6) the composition of the atmosphere under which the combustion takes place.

In the following pages we will discuss the contribution of the individual aspects focussed on by the specific experiments (indicated by the number in brackets according to the process scheme displayed in Fig. 2).

From the laboratory experiments and the outdoor samples, significant differences in the isotopic signature of the combustion-derived CO_2 become obvious. We deduce that a major impact of the obtained results has to be dedicated to the burned material itself, as the combustion process is largely regulated by the fuel specific composition, its structure and interactions with the environment.

The contribution of active fractionation is also determined by these prerequisites. Fractionation as an active process might be both temperature and gas flow speed related. Depending on the consumption of oxygen and the resulting air inflow, which determines the appearance of turbulent vs. laminar vs. diffusive motion, kinetic fractionation might appear. Thermal fractionation might become a factor due to temperature gradients which are developing around the flame at lower combustion temperatures.

3.1 Fuel material

When focussing on the impact and the interactions attributable to the individual components, the fuel material is central. A first differentiation between the studied fuels could be accomplished by visual comparisons of the smoke formation. It varied depending on the temperature, initialized for needles and heather at about 490 °C, wood ∼550 °C, peat and cellulose ∼600 °C and ends with only a small amount for coal at ∼650 °C. A sudden ignition of the degassed compounds and the supplied oxygen took place a few seconds later.

Isotope analysis of the combustion-derived CO_2 revealed a $\delta^{18}O$ variability of about 26‰ with a separation into three distinct groups (see Fig. 3): the heaviest oxygen isotopic signatures (that is, the least depleted compared to atmospheric oxygen) are formed by green plant parts (i.e. needles, heather). The intermediate group contains the wooden

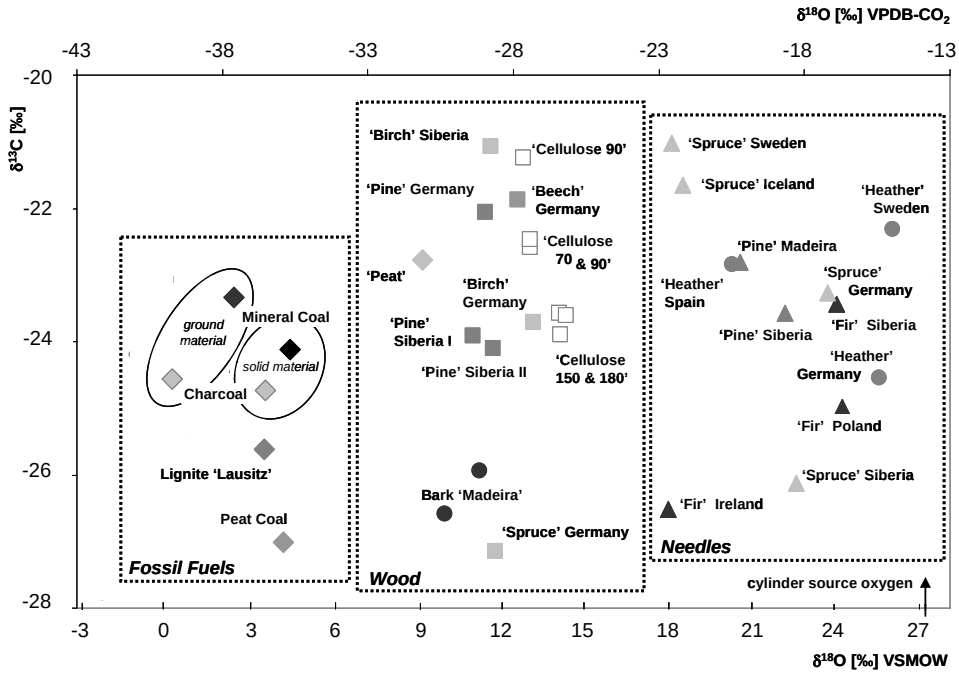

Fig. 3. Isotopic signature of combustion-derived CO_2 from various kinds of fuels of different spatial origin. Triangles indicate needle material, squares wood material, diamonds fossil fuels, the varied species are additionally marked by different hues. The numbers stated beside the cellulose samples refer to the amount of supported oxygen (see for details text section "environmental conditions").

material and the cellulose reference samples, while the third, most depleted group, comprises the fossil fuels.

As the chemical composition (Fig. 2, number 1) implies the inherent elements and defines by their amount and ratios the basic conditions for the reaction products and the energy content of the fuel, the mechanical properties (subsumed by 'structure' in Fig. 2, number 2) are modulating the burning progress. Heat conductance and the resulting progression of the combustion front-line are mainly affected by the density of the material and by the shape of the surface, while the ratio of 'surface to volume' defines the effective attacking area where volatile compounds are released and the thermally induced oxidation process takes its origin. The internal scaffolding determines the mechanic stability and thus influences the burning conditions from ignition to ultimate collapse.

The impact of the material's structure was examined by three specific test series:

1. The comparison of charcoal and coal which were combusted both as solid cubic samples and as ground material with small grain size (see Fig. 3): differences were about 3.3‰ for charcoal, 2.0‰ for coal and 6.3‰ for peat coal, with the CO_2 from ground material being more depleted.

2. The combustion of the (dry) compact cellulose rectangle for the "water experiment" versus the pairs of single stripes used for the common combustion (see Fig. 4): the fuel with the higher compactness is again less depleted in $\delta^{18}O$ by about 2.8‰ compared to the results from the reference material.

3. Effective differences could also be observed when relating the surface-volume ratios of the diverse needle material: for the spruce samples we found increasing needle surfaces from the German to the Swedish samples (measuring length, width and height of the needles, $n = 15$, and calculating the surface by using adapted formulas describing rods). Like in the previous case, we find that the bigger the surface, the more depleted in $\delta^{18}O$ is the derived CO_2 (see Fig. 3).

The observed variances between the solid and ground, that means the different surface-volume ratios, are for the $\delta^{18}O$ of the fossil fuels on the order up to 6.3‰ and for the needle material about 5.2‰. The latter concerns the difference between the samples "Iceland" and "Germany". Most probably, the following three aspects cause this behaviour: (1) the oxygen supply to the "point-of-reaction", which should be better for the enlarged surfaces, (2) the range of the affecting temperature, that should be narrower for the ground material while due to the slower movement of the fire front the kernel of the solid material is processed in a hotter environment than the outer skin, and (3) because of the concentrated release of volatile constitutes from the ground material the moment of

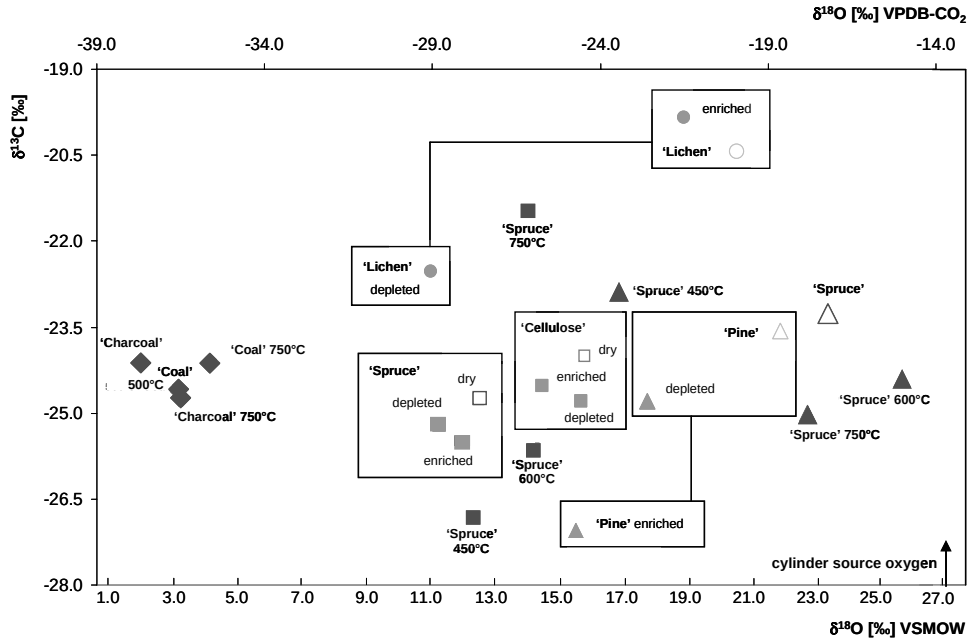

Fig. 4. Isotopic signature of combustion-derived CO_2 from experiments focussing on temperature relevance (dark symbols) and the impact of "plant moisture" (marked in boxes). Open symbols indicate the results from reference combustion runs at 750 °C. The different kind of material is marked as follows: diamonds = fossil fuels, squares = wood/cellulose, triangles = needles, circles = lichen.

ignition shall be earlier, i.e. when the temperature is on a lower level.

We found that CO_2 formed with limited heating (temperatures below 450–500 °C) tends to be more depleted in $\delta^{18}O$ than CO_2 that is derived from combustion at higher temperature (750–800 °C). The observed differences are about 0.9‰ for coal, 1.2‰ for charcoal, 1.7‰ for the spruce wood sample and 5.8‰ for the spruce needle sample (see Fig. 4).

A certain effect was also recognizable in the ^{13}C signatures derived from the combustion experiments performed under different temperature regimes. Studies by Turekian et al. (1998) indicated dependencies for the carbon isotopic signature from C_3 and C_4 plant material which should be mainly affected by differences in the degradation behaviour. Our results confirm this hypothesis, however without a clear tendency for all materials (see Fig. 4). The larger variability between the specific fuel materials in the ^{13}C compared to the ^{18}O signals might be partly caused by the addition of a second oxygen source (from the cylinder) that levels the ^{18}O signal in contrast to the ^{13}C values derived only from the fuel material "C" source. Since besides the specific material composition and structure all conditions are identical it can be deduced that the fuel material itself has a strong influence on the isotopic composition of the combustion-derived CO_2.

Another specific aspect we analyzed is the ratio of flammable and not combustible components. Highly volatile compounds act in a different way than those elements retrieved from the ash. Resulting effects can be seen in Fig. 3. A difference of about 9‰ in $\delta^{18}O$ between beech wood and charcoal (originating from beech wood) becomes obvious. During the charcoal production the material's composition is transformed under anaerobic conditions, whereby most of the volatile and highly flammable constituents are released. Due to this loss the ignition of charcoal occurs later and under different temperature conditions compared to the original wood material. A similar relation can be deduced from the comparison of needles and wood from the coniferous samples. Because of the relative higher content of volatile constituents inside the needles, the ignition and the onset of the combustion with an open flame take place earlier than for the wood material. From these we suppose that the timing of the thermal decomposition is a key aspect that determines the breakage of molecular bounds and the mobilisation of specific groups. When assuming great variances in the oxygen isotopic signature of different groups (Schmidt et al., 2001; Werner, 2003), significant variations might be therefore conceivable also in the resulting CO_2 and side products.

An important aspect affecting the timing of the thermal decomposition (that means also the setting when the combustion starts to become an endothermic process) is the "energy consumption" for heating and evaporation. The results displaying the influence of the moisture content are shown in Fig. 2 (number 5). When comparing the CO_2 data from combustion of dry material with material pickled either in depleted or in enriched water, a more or less distinct tendency towards larger depletion for the wet fuels is recognizable (see

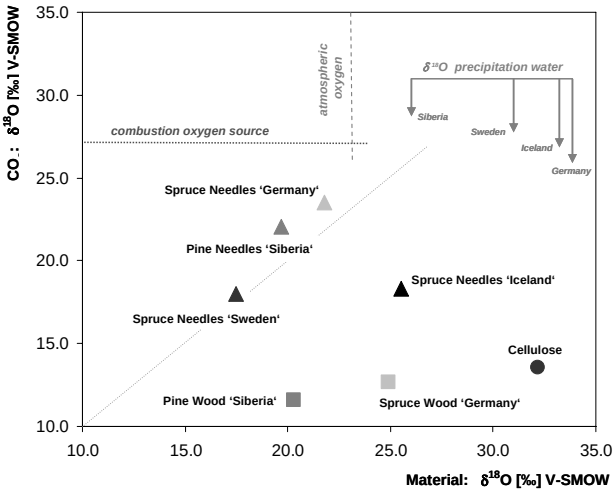

Fig. 5. Isotopic signature of the material's oxygen and the combustion-derived CO_2 (see also Table 2). Indicated are as well the isotopic signatures of the oxygen source of the combustion experiments (dark dotted line), the atmospheric molecular oxygen (vertical dashed line) and the oxygen signature of the precipitation water from the spatial origin of the bulk material samples (arrows; IAEA/WMO, 2006).

Fig. 4). This is because of the longer time span that the material is processed under lower temperature conditions. The wet-dry differences are about 0.9‰ for the spruce wood sample, 0.7‰ for cellulose, 6.2‰ for the pine needles and 5.6‰ for the lichen samples (using the averages of depleted and enriched wet samples).

By the fuel inherent oxygen (number 3 in Fig. 2) an important reactant for the combustion reaction can be released and applied right at the seat of fire. Since the fuel oxygen has a specific isotopic signature depending on the kind of material and the spatial origin, this might affect directly the combustion products. Table 2 displays the values for $\delta^{13}C$ and for $\delta^{18}O$ of different parts from singular trees grown in central Germany, northern Sweden, central Siberia, Iceland and of the cellulose reference material (IAEA-C3).

As shown in Fig. 5 the difference of the isotopic signatures from the combusted needle material originating from Germany and Sweden is nearly reflected in the derived CO_2 ($\delta^{18}O$ Germany 23.5‰ and $\delta^{18}O$ Sweden 18.0‰). However, the $\delta^{18}O$ is much more depleted for the needles from Iceland ($\delta^{18}O$ in CO_2 is 18.3‰); also ^{18}O in CO_2 from the wood samples, the cellulose samples and the fossil fuel samples is distinctly depleted as compared to the originating fuel. We assessed the contribution of fuel oxygen to the $\delta^{18}O$ in CO_2 by a two end-member mixing model comprising fuel oxygen and cylinder oxygen with a $\delta^{18}O$ value of 27.2‰. The expected $\delta^{18}O$ value for stoichiometric combustion of cellulose is 28.9‰ but the measured value is only 13.5‰. Slightly lower discrepancies can be deduced for the wood material samples from Germany (26.5‰ to 12.6‰) and Siberia (25.2‰ to 11.6‰). Isotopic fractionation of oxygen gas during diffusion to the flame is responsible for at least part of this effect, however, different fuel-specific chemical compositions might lead to different shares of (minor) products with again different oxygen isotope ratios.

Information about the influence of fuel inherent and applied oxygen on the isotopic signal can be concluded also from the direct comparison of the $\delta^{18}O$ values in CO_2 and H_2O. In Fig. 6 the measured isotopic signatures of four different kinds of material are displayed, soaked both in ^{18}O enriched and depleted water, together with the results from two dry reference samples.

While in the CO_2 signals for the individual material samples no distinct differences can be seen (except for the lichen samples for which the difference was 7.9‰), clear differences are obvious between the H_2O signatures: from about 10‰ for the "Spruce" sample to about 27‰ for the "Cellulose" and for the "Pinus" samples. All oxygen in the derived CO_2 is distinctly heavier than the oxygen signature of the water pickled in – in contrast to the combustion-derived H_2O values which are reflecting the base water signature (except the "Lichen enriched" and the "Pinus enriched" results). This clearly indicates a separation of the combustion-derived products due to different oxygen sources and reaction processes: the $\delta^{18}O$ in CO_2 is mainly originating from the bulk material, while the $\delta^{18}O$ in H_2O originates mainly from the "plant water". The discrepancies in the $\delta^{18}O$ H_2O signals between the different materials are most likely induced by material specific water fixation capabilities (lower for the needles compared with the cellulose material) and the release rate during the heating and ignition phase of the combustion process. This hypothesis is confirmed by the CO_2 results derived from the "Lichen" samples: it seems that the lichen became physiological active again after they were wetted and assimilated the oxygen directly from the water source into the plant material – indicated by the distinctly decreased CO_2 value from the sample pickled in the depleted water.

3.2 Combustion behaviour

Depending on the chemical and physical character of the fuel, a specific combustion behaviour can be observed. This subsumes the flammability, the style of disaggregating, the tendency to maintain a covering ash layer and the formation of smoke. By the evolution of a covering ash layer the admittance of oxygen to the combustion zone becomes restricted, as well as the formation of a smoke plume containing a high fraction of inflammable components inhibits the oxygen supply and the development of an open flame.

3.3 Environmental conditions

In addition to the parameters described so far, the atmosphere modulates the environmental conditions through changes in

Table 2. Isotopic values of needles and wood from singular trees grown in central Germany (Gifhorn), northern Sweden (Umeå), central Siberia (Zotino) and Iceland (Mývatn) and of cellulose reference material ($\delta^{13}C$ is given on the VPDB scale, $\delta^{18}O$ on the VSMOW scale).

	Needles		Wood			Needles		Wood	
	$\delta^{13}C$	$\delta^{18}O$	$\delta^{13}C$	$\delta^{18}O$		$\delta^{13}C$	$\delta^{18}O$	$\delta^{13}C$	$\delta^{18}O$
Picea	[]	[‰]	[‰]	[‰]	***Pinus***	[‰]	[‰]	[‰]	[‰]
Germany	−26.0	21.3	−20.0	25.1	Siberia	−19.6	19.7	−15.9	20.3
	−25.4	21.6	−19.9	24.9		−19.7	19.9	−15.8	20.2
	−26.3	21.5	−20.0	24.8		−19.4	19.6	−15.7	20.3
Mean	***−25.9***	***21.5***	***−20.0***	***24.9***		***−19.6***	***19.7***	***−15.8***	***20.3***
Std.dev.	*0.46*	*0.15*	*0.06*	*0.15*		*0.15*	*0.15*	*0.10*	*0.06*
Sweden	−23.0	17.5	−17.7	23.8					
	−23.1	17.6	−17.8	23.0					
	−23.2	17.4	−17.8	23.1					
Mean	***−23.1***	***17.5***	***−17.8***	***23.3***					
Std.dev.	*0.10*	*0.10*	*0.06*	*0.44*					
								δ^{13}**C**	δ^{18}**O**
								[‰]	[‰]
Iceland	−20.1	25.5					**Cellulose**	−16.8	32.2
	−19.9	25.4						−16.6	32.3
	−20.4	25.5						−16.6	32.2
Mean	***−20.1***	***25.5***						***−16.7***	***32.2***
Std.dev.	*0.25*	*0.06*						*0.10*	*0.06*

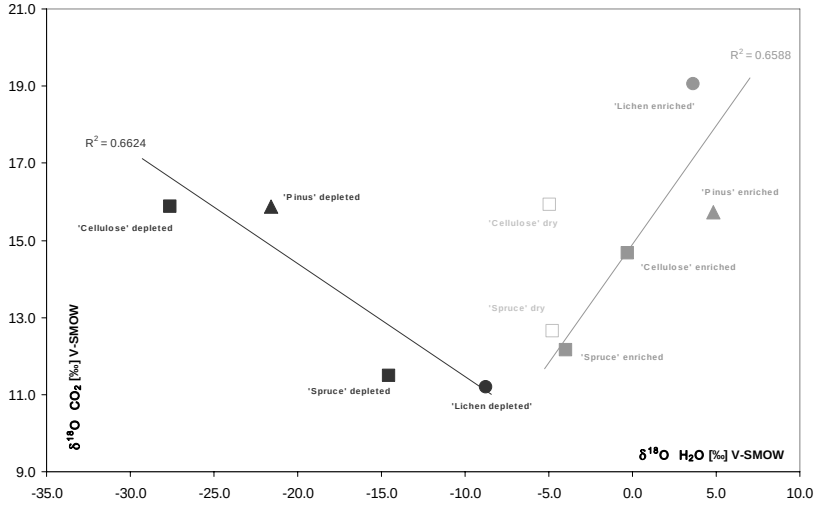

Fig. 6. Isotopic signature of the combustion-derived CO_2 and H_2O from four different kinds of fuel (black symbols are samples wetted with the depleted water, grey ones with the enriched water). The open symbols refer to the combustion signatures of the dry reference substance from which we received a sufficient amount of combustion water for analysing ("Spruce" and "Cellulose"). Values are given on the VSMOW scale.

wind speed, humidity and temperature as well as additional reactants like N_2, CH_4, etc. (number 3 and 6 in Fig. 2). The supply of oxygen to the process zone, as well as the removal of the smoke, is under natural conditions determined by thermal updraft and wind. We tried to simulate these effects by the modulation of the oxygen flow. To investigate the influence of the oxygen availability we combusted a cellulose series supplied with a decreasing amount of oxygen (see Fig. 3), performed the combustion of natural gas with different addition of oxygen and obtained data by the samples using ambient atmospheric air (see also Fig. 7). A clear trend towards the ^{18}O signature of the used oxygen from the

Table 3. Isotopic values of fuel material, combustion derived CO_2 and H_2O, source oxygen, source water and precipitation from measurement sites close to the geographical origin of selected fuel material.

Sample	$C^{18}OO$ (V-SMOW)	^{18}O Material (V-SMOW)	$C^{18}OO$ (VPDB-CO_2)	$^{13}CO_2$	$H_2^{18}O$	Deuterium	Material	Figure
'Fir' Siberia	23.87		−16.89	−23.45			needles	3
'Fir' Ireland	17.85		−22.67	−26.52			needles	3
'Fir' Poland	24.06		−16.71	−24.99			needles	3
'Spruce' Iceland	18.38	25.5	−22.16	−21.65			needles	3, 5
'Spruce' Sweden	17.96	17.5	−22.57	−21.02			needles	3, 5
'Spruce' Germany	23.54	21.8	−17.21	−23.27			needles	3, 4, 5
'Spruce' Siberia	22.43		−18.28	−26.13			needles	3
'Spruce' 450 °C	17.05		−23.44	−22.91			needles	4
'Spruce' 600 °C	25.85		−14.99	−24.45			needles	4
'Spruce' 750 °C	22.90		−17.83	−25.01			needles	4
'Pine' Siberia	22.04	19.7	−18.65	−23.58			needles	3, 4, 5
'Pine' Madeira	20.39		−20.23	−22.82			needles	3
'Pine' enriched	15.72		−24.72	−27.07	4.84	−66.0	needles	4, 6, 8
'Pine' depleted	17.93		−22.6	−25.88	−21.58	−229.6	needles	4, 6, 8
'Beech' Gifhorn	12.46		−27.84	−21.88			wood	3
'Birch' Gifhorn	13.00		−27.32	−23.71			wood	3
'Birch' Siberia	11.48		−28.79	−21.08			wood	3
'Pine' Gifhorn	11.30		−28.96	−22.05			wood	3
'Pine' Siberia I	10.87		−29.37	−23.91			wood	3
'Pine' Siberia II	11.56	20.3	−28.71	−24.10			wood	3, 5
'Spruce' Germany	11.68		−28.6	−27.14			wood	3
'Spruce' 450 °C	12.52		−27.79	−26.85			wood	4
'Spruce' 600 °C	14.39		−26.00	−25.63			wood	4
'Spruce' 750 °C	14.23		−26.15	−21.48			wood	4
'Spruce' dry	12.64	24.9	−27.67	−24.85	−4.76	−137.0	wood	4, 5, 8
'Spruce' enriched	12.17		−28.13	−25.53	−3.98	−57.8	wood	4, 6, 8
'Spruce' depleted	11.49		−28.78	−25.21	−14.55	−222.6	wood	4, 6, 8
'Heather' Sweden	25.89		−14.95	−22.32			heather	3
'Heather' Germany	25.40		−15.42	−24.55			heather	3
'Heather' Spain	20.14		−20.47	−22.84			heather	3
Bark 'Madeira'	9.85		−30.35	−26.59			bark	3
Bark 'Madeira'	11.10		−29.15	−25.94			bark	3
'Lichen enriched'	19.06		−21.51	−19.85	3.61	−36.2	lichen	4, 6, 8
'Lichen depleted'	11.20		−29.05	−22.53	−8.73	−177.7	lichen	4, 6, 8
'Cellulose 70 & 90'	12.92		−27.41	−22.47			reference	3
'Cellulose 70 & 90'	12.90		−27.43	−22.59			reference	3, 7
'Cellulose 90'	12.66		−27.65	−21.24			reference	3
'Cellulose 150 & 180'	14.01		−26.36	−23.89			reference	3
'Cellulose 150 & 180'	13.94		−26.43	−23.57			reference	3, 5, 7
'Cellulose 150 & 180'	14.20		−26.17	−23.61			reference	3
'Cellulose' dry	15.92		−24.52	−24.09	−4.92	−86.7	reference	4, 8
Cellulose (O_2 atmo.)	19.47		−21.12	−21.58			reference	7
'Cellulose' enriched	14.66		−25.73	−24.52	−0.26	−89.3	reference	4, 6, 8
'Cellulose' depleted	15.87		−24.57	−24.80	−27.61	−261.6	reference	4, 6, 8
Cellulose	13.54	32.2					reference	5
Mineral Coal (ground material)	2.3		−37.60	−23.33			fossil fuel	3
Mineral Coal (solid material)	4.29		−35.69	−24.12			fossil fuel	3, 4
'Coal' 500 °C	3.35		−36.60	−24.63			fossil fuel	4
Charcoal (ground material)	0.09		−39.72	−24.56			fossil fuel	3
Charcoal (solid material)	3.44		−36.51	−24.72			fossil fuel	3, 4, 7
'Charcoal' 500 °C	2.21		−37.69	−24.13			fossil fuel	4
Lignite 'Lausitz'	3.38		−36.57	−25.61			fossil fuel	3
Peat Coal (Slovakia)	4.08		−35.89	−27.01			fossil fuel	3
Peat coal (Ireland)	10.35		−29.88	−22.74			fossil fuel	7
'Peat'	9.06		−31.11	−22.77			fossil fuel	3
Charcoal (O_2 atmo.)	22.54		−18.17	−23.37			fossil fuel	7
Peat Coal (O_2 atmo.)	19.28		−21.30	−24.43			fossil fuel	7

Table 3. Continued.

Sample	$C^{18}OO$ (V-SMOW)	^{18}O Material (V-SMOW)	$C^{18}OO$ (VPDB-CO_2)	$^{13}CO_2$	$H_2^{18}O$	Deuterium	Material	Figure
Diesel Bus	23.80		−16.96	−27.21			fossil fuel	7
Diesel Bus	26.04		−14.81	−27.37			fossil fuel	7
Diesel Car	22.24		−18.46	−27.29			fossil fuel	7
Gasoline cold engine	29.63		−11.36	−26.57			fossil fuel	7
Gasoline	26.02		−14.83	−28.77			fossil fuel	7
Gasoline	26.36		−14.50	−28.66			fossil fuel	7
Natural gas (O_2 deficit)	13.72		−26.64	−31.75			fossil fuel	Text 3.3
Natural gas (O_2 optimal)	12.63		−27.68	−28.99			fossil fuel	Text 3.3
Natural gas (O_2 excess)	10.40		−29.83	−29.72			fossil fuel	Text 3.3
Atmosphere	23.76		−17.00				O_2 source	7
Gas cylinder	27.23		−13.66				O_2 source	7
'GS46' Antarctica					−43.70	−376.1	water source	8
'GS49' Atlantic Ocean					−0.39	28.2	water source	8
Gifhorn/Germany	33.84		−7.31				precipitation	5
Sweden	31.00		−10.04				precipitation	5
Siberia	25.98		−14.86				precipitation	5
Iceland	33.17		−7.96				precipitation	5

cylinder (27.2‰ VSMOW) is recognizable from the combustion series of natural gas with (a) an excess of oxygen, (b) the optimal stoichiometric amount and (c) a deficit of oxygen – that is correlated with the decreasing oxygen availability ($\delta^{18}O$ of (a) 10.4‰, (b) 12.6‰ and (c) 13.7‰; not shown in the figures). That means, when the oxygen supply is high, fractionation can easily take place, while with decreasing oxygen amount relatively more of the heavier isotope is used for the combustion, getting closer to the assumed full usage of oxygen, which would directly transfer the oxygen isotopic ratios into CO_2.

However, the variation of oxygen supply in the cellulose series (see Fig. 3) did not show a similar relation in $\delta^{18}O$ and also not such pronounced differences. The samples derived from the combustion with oxygen excess are by about 1.4‰ less depleted in relation to the source oxygen than the ones obtained with the reduced oxygen availability.

A stronger correlation seems to exist with respect to the $\delta^{13}C$ signature (total range of 2.7‰). At least two groups can be distinguished: a more depleted one containing samples derived from combustion with the higher oxygen availability, compared to a less depleted one formed when reducing the oxygen throughput. But also the $\delta^{13}C$ data do not show a uniform relationship, indicated by the difference between the two samples derived with the identical oxygen support (marked with "Cellulose 90").

Information regarding the combustion under real atmospheric conditions was obtained from the direct sampling of car exhaust and the laboratory combustion of solid material utilizing ambient air (see Fig. 7). Compared to the samples derived from the combustion with pure oxygen supply (which is 3.4‰ more enriched than the ambient air source) the results from the combustion with ambient air are characterized by CO_2 distinctly less depleted in $\delta^{18}O$ (by 5.3‰ for cellulose, 8.9‰ for peat coal and 19.1‰ for charcoal). Also the outdoor results for the liquid fossil fuels show only a narrow range of about 7‰ between the samples of cars with gasoline motors, two local-traffic busses and a car with a diesel engine.

These data support the hypothesis about a dampening influence of the natural atmosphere. Additional reactants involved into the combustion process, like nitrogen (which contributes with 78% to the atmospheric air), counteracts the combustion since these elements might react with O_2 themselves, or they might react faster with the fire-released compounds than the oxygen. Further on, a certain amount of energy is needed for heating a bigger, non reactive amount of gas which leads to a decrease in the combustion temperature.

Humidity and temperature also influence the combustion processes. Water vapour from fuel or humid air may cool the combustion gases and affect chemical reactions between reactants and products, for example, through isotope exchange with condensing water.

3.4 Combustion process

The combustion process is determined by the fuel material, its specific combustion behaviour and the environmental conditions (see Fig. 2). The combustion process consists of three regimes: (1) degassing and ignition, (2) combustion with open flame, and (3) glowing/smoldering. When looking at a burning object it becomes obvious that all three steps are present at the same time. Thus we have to consider that the formed CO_2 represents integral information.

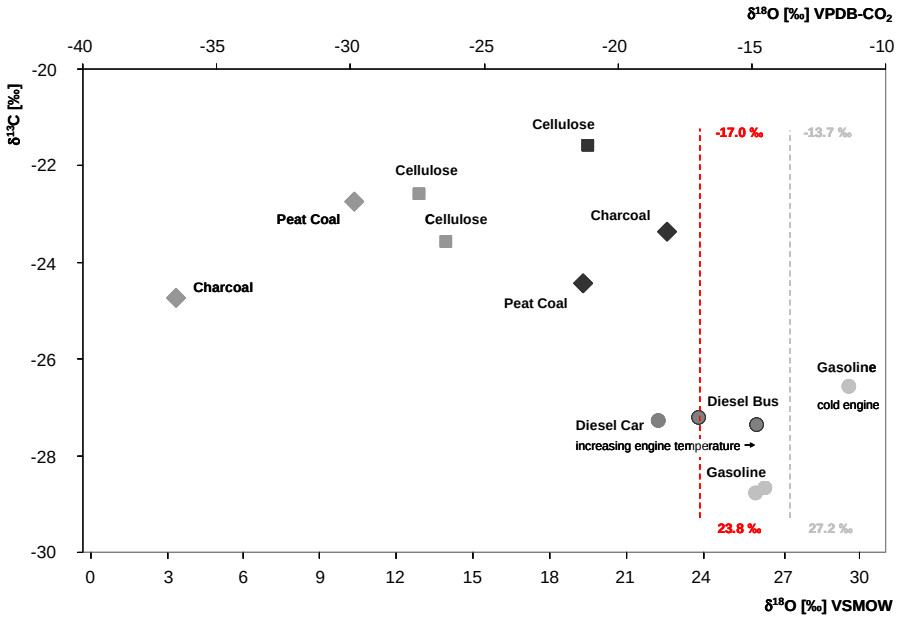

Fig. 7. Isotopic signature of the used oxygen sources (dotted lines: 27.2‰ dedicated to the pure oxygen cylinder, and 23.8‰ to the ambient air source) and of the combustion-derived CO_2. The samples which originate from combustion with ambient air are indicated by circles (car exhaust), and by the black symbols (solid material, laboratory study). In contrast the light grey symbols denote the combustion results of the solid material with the pure oxygen source.

Two factors mainly influence the combustion process: the temperature and the "rate of combustion". When burning happens at low rate of combustion a sufficient amount of atmospheric oxygen can reach the seat of fire in time. Constraining conditions like the presence of an ash layer or the formation of dense smoke (CO_2, H_2O and other combustion products) on the other hand may promote the influence of the fuel oxygen to the ^{18}O signal in the derived CO_2.

At the beginning of the combustion event the temperature reflects the quantum of endothermic energy that has to be provided to exceed the threshold for an ignition. As it became already obvious from some of the experiments discussed before, the moment of ignition seems to be of high importance. But also when the burning is in process a depression of the heat production can counteract subsequent processes, for instance due to energy consumption for the evaporation of moist material. This is reflected by the combustion efficiency, i.e. the ratio of carbon released in form of CO_2 to the carbon amount of the other combustion products. During incomplete combustion, as it takes place as well in the degassing stage, the fraction of produced CO_2 is low while the formation of constituents like CO and CH_4 is high. From Fig. 4 it becomes obvious that CO_2 derived from combustion with temperatures below 600 °C is depleted in ^{18}O compared to CO_2 formed at temperatures above 600 °C. Since the ^{18}O of the reactants has to be found in one of the products we assume that the heavier oxygen is preferentially accumulated in less processed constitutes, such as CO, or the air oxygen. When the combustion temperature increases, CO can be converted by a second reaction step into CO_2, and this ^{18}O pool becomes part of the (now slightly more enriched) CO_2 signal that is reflected by the data from the 750 °C experiment. A similar process is described by Chanton et al. (2000) for the carbon isotopic signatures of methane derived from combustion and biomass burning.

To initiate or to force certain reactions it is necessary to reach, by the combustion process, a minimum temperature. For example, the reaction equilibrium for $C + CO_2 \leftrightarrows 2\ CO$ is shifted to the product side at temperatures >600 °C. In the temperature range from about 800 °C NO_x can be formed, and it needs about 1250 °C to oxidize atmospheric nitrogen.

With respect to the influence of very high temperatures combined with the utilisation of atmospheric air, information can be gained from the sampling of the exhaust gases from cars and busses. The results shown in Fig. 7 indicate for the diesel vehicles a relative increase of ^{18}O in the derived CO_2 coming along with increasing engine temperatures, as described before for the plant and fossil fuel material. The obtained result from the hot car engine is in a similar order of about 26.0‰ VSMOW as derived from the warmest diesel engine. However, in contrast the heaviest signature from the gasoline cars originates from the cold engine sampled just after starting. This discrepancy might be due to several reasons. The ^{18}O depletion in diesel car exhaust coming along with decreasing temperatures can be attributed to incomplete reactions, while the heavy isotopic signature derived from the

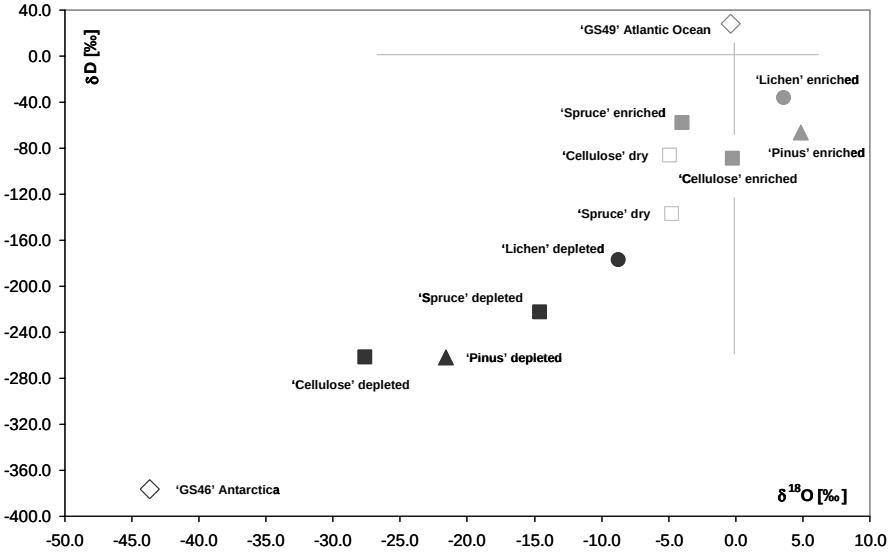

Fig. 8. Isotopic signature of the used water sources (open diamonds) and of the combustion-derived H_2O from four different kinds of fuel (black symbols are samples wetted with the depleted water, grey ones with the enriched water). The open symbols refer to the dry substance. Values are given on the VSMOW scale.

cold gasoline car might be at least partly an effect caused by the still non-active catalytic converter. An explanation for the general difference between the results derived from the diesel and gasoline engines is evident due to the different technical principles: in contrast to gasoline engines diesel aggregates run by a lean fuel-to-air mixture (Lambda > 1), this means that not all oxygen is consumed during the combustion process which allows for a higher degree of fractionation processes.

3.5 Side products

Because of suboptimal combustion conditions, and the presence of elements other than carbon and oxygen, a variety of other products than CO_2 is formed during combustion processes. These side products can be divided into four groups: unconsumed oxygen, compounds which are containing oxygen, aerosols without oxygen and remaining products like ash or soot. With respect to the differentiation of individual processes causing the diverging ^{18}O signals in combustion-derived CO_2, further essential information became available through the analyses of these side products.

One factor we examined specifically was the isotopic signature of H_2O derived from the combustion process. Displayed in Fig. 8 are the obtained δD and $\delta^{18}O$ values of the samples as well as of the source water. Even if no distinct differentiations became obvious in the CO_2 signal from material moistened by strongly depleted and enriched water (see again Fig. 4), significant ^{18}O signals could be obtained from the analysis of the derived combustion water. While the results of the samples labelled by the water from the Atlantic Ocean ("enriched") are clustered within a narrow band (of about 10‰ in $\delta^{18}O$ and 53‰ in δD) the difference between the samples soaked with water from Antarctica ("depleted") was about 19‰ in $\delta^{18}O$ and 84‰ in δD. From a linear regression intercept applied through the combustion-derived data a relatively high correlation is recognizable ($R^2 = 0.87$). However, there is also a distinct offset regarding the values of the source waters, indicated by the obvious gap between the signature of the Antarctic input water and the results from the combustion of the material.

The most interesting information can be deduced from the "cellulose dry" and "spruce dry" results. When one compares for the wood material the differences between the bulk $\delta^{18}O$ (24.9‰ VSMOW, see Table 2, *Picea Germany*) and the $\delta^{18}O$ from the CO_2 samples (12.6‰ VSMOW, see Fig. 4), a relative isotope ratio difference of about 12.1‰ can be recognized. Depletion relative to the bulk $\delta^{18}O$ and the $\delta^{18}O$ of the oxygen from the cylinder (27.2‰ VSMOW) takes also place in the combustion-derived water with a value of −4.8‰ VSMOW (Fig. 8). Assuming that only CO_2 and H_2O are formed by the combustion (in nearly equal ratios: 6 mol CO_2 and 5 mol H_2O per mol cellulose) a total deviation can be calculated from the expected result on the order of about −31‰. Therefore also the formation of other side products (like CO and CH_4 from low temperature processes, or NO_x formed under high temperature conditions), and a contribution from the residual oxygen has to be taken into consideration to obtain a closed ^{18}O balance. Kato et al. (1999) describe an enrichment of approximately 3‰ in the $\delta^{18}O$ of CO derived from biomass burning at flaming stage relative to the $\delta^{18}O$ of the ambient air. We see from our experiments

that: since (1) CO is formed only in a small fraction during efficient combustion (compared to CO_2), (2) the amount of nitrogen involved into the process can be neglected (due to the supply with pure O_2 from the cylinder), (3) CO_2 and H_2O are insufficient sinks (as discussed above), and (4) no solid material remained from the burning the most probable sink of the "missing ^{18}O" is the unconsumed oxygen fraction. That means that a strong fractionation takes place when the ambient oxygen is incorporated in the combustion process (entering the reaction zone, forming of CO_2, H_2O, CO, etc.), whereby the lighter isotopes are predominantly processed – leaving the heavier isotopes in the surplus oxygen fraction.

To assess these contributions to the final isotopic CO_2 signal, the examination of changes between the $\delta^{18}O$ of the input oxygen and the unconsumed oxygen leaving the combustion zone will be mandatory. Mind, however, that due to the large amount of oxygen, as compared to CO_2, the isotopic effect will still be very small. Because of technical limitations this experiment could not be performed but we highly recommend to continue with research in this direction.

4 Conclusions

When comparing the combustion-derived $CO^{18}O$-signal from different kinds of fuel material that were combusted in the laboratory under optimal and identical conditions, significant effects were recognized. Dependencies could be observed with respect to specific process conditions, such as combustion temperature, material structure, and composition of the air available for burning. The series of experiments showed that the isotopic signature of combustion-derived CO_2 is highly variable and depends on several key parameters and their complex interactions.

The evaluation of our results' relevance to the (expected) signal in atmospheric measurements and their impact for modelling studies is complex. Even such huge deviations from the so far assumed $CO^{18}O$ signature as seen during our laboratory combustion experiments most probably have no significant impact on the global pattern of the CO_2 oxygen isotopic signal in simulation studies (Cuntz et al., 2003; M. Cuntz, personal communication, 2008). The reason for this is the fast oxygen isotope exchange of CO_2 with the much larger water oxygen reservoir. However, individual isotopic compositions surely have effects which are not negligible in the context of local to regional investigations and discrete air sampling for data acquisition. In consequence, this inaccuracy will be introduced indirectly into modelling studies when using data obtained in local and regional studies as input or validation information.

We suggest that natural combustion processes, leading to a local, not sustained depletion of ^{18}O in the formed CO_2, on the long term might enrich ^{18}O in atmospheric molecular oxygen. This would then contribute to the not yet fully understood Dole-effect (e.g. Dole et al., 1954; Bender et al., 1994; Hoffmann et al., 2004).

In order to get a comprehensive understanding of the isotopic effects and contributions of combustion processes, this investigation was a first step that needs to be succeeded by further studies. Direct observations, within and in the vicinity of smoke and exhaust plumes of wildfires and anthropogenic combustion sources, are just as desirable as enhanced laboratory studies focussing on the isotopic signature of the compounds concurrently released with the CO_2.

Acknowledgements. We are grateful to A. T. Aerts-Bijma, B. A. M. Kers, J. K. Schut, H. J. Streurman and B. M. A. A. Verstappen-Dumoulin for technical assistance, to a numerousness of persons, as well as British Petroleum (BP) and Shell Marine Fuel (Hamburg), who supported the study by submitting fuel material. MS likes to thank the European Science Foundation (ESF) programme "Stable Isotopes in Biospheric-Atmospheric Exchange (SIBAE)" to enable the lab studies at the University of Groningen by awarded exchange grants.

Last not least we wish to thank the Editor and one anonymous referee for their substantial contributions greatly improving the clarity and legibility of the presentation.

The service charges for this open access publication have been covered by the Max Planck Society.

Edited by: J. Kaiser

References

Bender, M., Sowers, T., and Labeyrie, L.: The Dole effect and its variations during the last 130.000 years as measured in the Vostok ice core, Global Biogeochem. Cy., 3, 363–376, 1994.

Burk, R. L. and Stuiver, M.: Oxygen Isotope Ratios in Trees Reflect Mean Annual Temperature and Humidity, Science, 211, 1417–1419, 1981.

Buhay, W. M., Wolfe, B. B., Elgood, R. J., and Edwards, T. W. D.: A report on the $\delta^{18}O$ measurements of the IAEA cellulose intercomparison material IAEA-C3, in: Reference and intercomparison materials for stable isotopes of light elements, Proceedings of a consultants meeting held in Vienna, 1–3 December 1993, IAEA-TECDOC-825, IAEA, Vienna, 165 pp., 1995.

Chanton, J., Rutkowski, C., Schwartz, C., Ward, D., and Boring, L.: Factors influencing the stable carbon isotopic signature of methane from combustion and biomass burning, J. Geophys. Res., 105, 1867–1877, 2000.

Ciais, P. and Meijer, H. A. J.: The $^{18}O/^{16}O$ isotope ratio of atmospheric CO_2 and its role in global carbon cycle research, in: Stable Isotope - Integration of biological, ecological and geochemical processes, edited by: Griffiths, H., BIOS Scientific Publishers, 409–431, 1998.

Ciais, P., Denning, A. S., Tans, P. P. Berry, J. A., Randall, D. A., Collatz, G. J., Sellers, P. J., White, J. W .C., Trolier, M., Meijer, H. A. J., Francey, R. J., Monfray, P., and Heimann, M.: A three-dimensional synthesis study of $\delta^{18}O$ in atmospheric CO_2: 1. Surface fluxes, J. Geophys. Res., 102, 5857–5872, 1997a.

Ciais, P., Tans, P. P., Denning, A. S., Francey, R. J., Trolier, M., Meijer, H. A. J., White, J. W. C., Berry, J. A., Randall, D. A., Collatz, G. J., Sellers, P. J., Monfray, P., and Heimann, M.: A

three-dimensional synthesis study of $\delta^{18}O$ in atmospheric CO_2 : 2. Simulations with the TM2 transport model, J. Geophys. Res., 102, 5873–5883, 1997b.

Coplen, T. B.: Normalization of oxygen and hydrogen isotope data, Chem. Geol., 72, 293–297, 1988.

Cuntz, M., Ciais, P., Hoffmann, G., Allison, C. E., Francey, R. J., Knorr, W., Tans, P. P., White, J. W. C., and Levin, I.: A comprehensive global three-dimensional model of $\delta^{18}O$ in atmospheric CO_2: 2. Mapping the atmospheric signal, J. Geophys. Res., 108(D17), 4528, doi:10.1029/2002JD003154, 2003.

Damoah, R., Spichtinger, N., Forster, C., James, P., Mattis, I., Wandinger, U., Beirle, S., Wagner, T., and Stohl, A.: Around the world in 17 days – hemispheric-scale transport of forest fire smoke from Russia in May 2003, Atmos. Chem. Phys., 4, 1311–1321, doi:10.5194/acp-4-1311-2004, 2004.

Dole, M., Lane, G. A., Rudd, D. P., and Zaukelies, D. A.: Isotopic composition of atmospheric oxygen and nitrogen, Geochim. Cosmochim. Ac., 6, 65–78, 1954.

Farquhar, G. D., Lloyd, J., Taylor, J. A., Flanagan, L. B., Syvertsen, J. P., Hubick, K. T., Wong, S. C., James R., and Ehleringer, J. R.: Vegetation effects on the isotope composition of oxygen in atmospheric CO_2, Nature, 363, 439–443, 1993.

Francey, R. J. and Tans, P. P.: Latitudinal variation in oxygen-18 of atmospheric CO_2, Nature, 327, 495–497, 1987.

Gehre, M. and Strauch, G.: High-temperature elemental analysis and pyrolysis techniques for stable isotope analysis, Rapid Commun. Mass Sp., 17, 1497–1503, 2003.

Gehre, M., Geilmann, H., Richter, J., Werner, R. A., and Brand, W. A.: Continuous Flow 2H/1H and ^{18}O /^{16}O Analysis of Water Samples with Dual Inlet Precision, Rapid Commun. Mass Sp., 18, 2650–2660, 2004.

Gemery, P. A., Trolier, M., and White, J.: Oxygen isotope exchange between carbon dioxide and water following atmospheric sampling using glass flasks, J. Geophys. Res., 101, 14415–14420, 1996.

Goldammer, J. G. and Furyaev, V. V.: Fire in Ecosystems of Boreal Eurasia, Kluwer Academic Publishers, Dordrecht, 390 pp., 1996.

Hao, W. M. and Liu, M.-H.: Spatial and temporal distribution of tropical biomass burning, Global Biogeochem. Cy., 8, 495–503, 1994.

Hoffmann, G., Cuntz, M., Weber, C., Ciais, P., Friedlingstein, P., Heimann, M., Jouzel, J., Kaduk, J., Maier-Reimer, E., Seibt, U., and Six, K.: A model of the Earth's Dole effect, Global Biogeochem. Cy., 18, GB1008, doi:10.1029/2003GB002059, 2004.

IAEA/WMO: Global Network of Isotopes in Precipitation. The GNIP Database, available at: http://isohis.iaea.org, 2006

IEA: International Energy Agency, Statistics of energy consumption, available at: http://www.iea.org, 2005.

IPCC: Climate Change 2007: The Physical Science Basis. Contribution of Working Group I to the Fourth Assessment Report of the Intergovernmental Panel on Climate Change, edited by: Solomon, S., Qin, D., Manning, M., Chen, Z., Marquis, M., Averyt, K. B., Tignor, M., and Miller, H. L., Cambridge University Press, Cambridge, United Kingdom and New York, NY, USA, 996 pp., 2007.

Kasischke, E. S., Hyer, E. J., Novelli, P. C., Bruhwiler, L. P., French, N. H. F., Sukhinin, A. I., Hewson, J. H., and Stocks, B. J.: Influences of boreal fire emissions on Northern Hemisphere atmospheric carbon and carbon monoxide, Global Biogeochem. Cy., 19, GB1012, doi:10.1029/2004GB002300, 2005.

Kato, S., Akimoto, H., Röckmann, T., Bräunlich, M., and Brenninkmeijer, C. A. M.: Stable isotopic compositions of carbon monoxide from biomass burning experiments, Atmos. Environ., 33, 4357–4362, 1999.

Kituyi, E., Marufu, L., Wandiga, S. O., Jumba, I. O., Andreae, M. O., and Helas, G.: Biofuel availability and domestic use patterns in Kenya, Biomass Bioenerg., 20, 71–82, 2001.

Kroopnick, P. and Craig, H.: Atmospheric Oxygen: Isotopic Composition and Solubility Fractionation, Science, 175, 54–55, 1972.

Langenfelds, R. L., Francey, R. J., Pak, B. C., Steele, L. P., Lloyd, J., Trudinger, C. M., and Allison, C. E.: Interannual growth rate variations of atmospheric CO_2 and its $\delta^{13}C$, H_2, CH_4, and CO between 1992 and 1999 linked to biomass burning, Global Biogeochem. Cy., 16, 1048, doi:10.1029/2001GB001466, 2002.

Ludwig, J., Marufu, L. T., Huber, B., Andreae, M. O., and Helas, G.: Domestic Combustion of Biomass Fuels in Developing Countries: A Major Source of Atmospheric Pollutants, J. Atmos. Chem., 44 , 23–37, 2003.

Meijer, H. A. J., Neubert, R. E. M., and Visser, G. H.: Cross contamination in dual inlet isotope ratio mass spectrometers, Int. J. Mass Spectrom., 198, 45–61, 2000.

Olsen, J., Seierstad, I., Vinther, B., Johnsen, S., and Heinemeier, J.: Memory effect in deuterium analysis by continuous flow isotope ratio measurement, Int. J. Mass Spectrom., 254, 44–52, 2006.

Page, S. E., Siegert, F., Rieley, J. O., Boehm, H.-D. V., Jaya, A., and Limin, S.: The amount of carbon released from peat and forest fires in Indonesia during 1997, Nature, 420, 61–65, 2002.

Pataki, D. E., Bowling, D. R., and Ehleringer, J. R.: Seasonal cycle of carbon dioxide and its isotopic composition in an urban atmosphere: Anthropogenic and biogenic effects, J. Geophys. Res., 108, 4735, doi:10.1029/2003JD003865, 2003.

Prentice, I. C., Heimann, M., and Sitch, S.: The carbon balance of the terrestrial biosphere: Ecosystem models and atmospheric observations, Ecol. Appl., 10, 1553–1573, 2000.

Schmidt, H .L., Werner, R. A., and Rossmann, A.: ^{18}O Pattern and biosynthesis of natural plant products, Phytochemistry, 58, 9–32, 2001.

Schumacher, M.: Airborne and Ground Level Flask Sampling for Regional Carbon Budgets – The Potential of Multiple Tracer and Isotope Analyses, PhD Thesis, University of Hamburg, Hamburg, 2005.

Sternberg L. S. L.: Oxygen and hydrogen isotope ratios in plant cellulose: Mechanisms and applications, in: Stable Isotopes in Ecological Research, edited by: Rundel, P. W., Ehleringer, J. R., and Nagy, K. A., Springer Verlag, New York, 124–141, 1989.

Turekian, V. C., Macko, S., Ballentine, D., Swap, R. J., and Garstang, M.: Causes of bulk carbon and nitrogen isotopic fractionations in the products of vegetation burns: laboratory studies, Chem. Geol., 152, 181–192, 1998.

USGS: Compilation of Minimum and Maximum Isotope Ratios of Selected Elements in Naturally Occurring Terrestrial Materials and Reagents, U.S. Geological Survey Water-Resources Investigations Report 01-4222, 2002.

van der Werf, G. R., Randerson, J. T., Giglio, L., Collatz, G. J., Kasibhatla, P. S., and Arellano Jr., A. F.: Interannual variability in global biomass burning emissions from 1997 to 2004, Atmos. Chem. Phys., 6, 3423–3441, doi:10.5194/acp-6-3423-2006, 2006.

Werner, R. A.: The online $^{18}O/^{16}O$ analysis: development and application, Isot. Environ. Healt. S., 39, 85–104, 2003.

Werner, R. A. and Brand, W. A.: Referencing strategies and techniques in stable isotope ratio analyses, Rapid Commun. Mass Sp., 15, 501–519, 2001.

Yakir, D.: Oxygen-18 of leaf water: a crossroad for plant-associated isotopic signals, in: Stable Isotope – Integration of biological, ecological and geochemical processes, edited by: Griffiths, H., BIOS Scientific Publishers, 1147–1168, 1998.

Zimnoch, M.: Investigation of isotopic composition of carbon dioxide in the environment, PhD Thesis (in Polish), University of Mining and Metallurgy, Krakow, 1996.

Zimnoch, M., Florkowski, T., Necki, J. M., and Neubert, R. E. M.: Diurnal variability of $\delta^{13}C$ and $\delta^{18}O$ of atmospheric CO_2 in the urban atmosphere of Krakow, Poland, Isot. Environ. Healt. S., 40, 129–143, 2004.